

# Substrate effects on domain structures of PZT 30/70 sol-gel films via PiezoAFM

S. Dunn\*, R.W. Whatmore

*Building 70, Nanotechnology, Cranfield University, Cranfield MK43 0AL, UK*

Received 8 May 2001; accepted 9 July 2001

## Abstract

Using an atomic force microscope (AFM) modified to perform PiezoAFM we have investigated the piezoelectric response of sol-gel thin film lead zirconate titanate (PZT 30/70,  $\text{PbZr}_{0.3}\text{Ti}_{0.7}\text{O}_3$ ) on Pt–Ti/SiO<sub>2</sub>/Si, indium tin oxide (ITO)/glass and Pt/MgO. The films were produced by spin coating a PZT 30/70 sol and firing at 520 °C for Pt electrode systems and 600 °C for the ITO system. By conducting PiezoAFM hysteresis loops we have shown that the localised piezoelectric response varies for PZT on differing substrates. The degree of asymmetry in the hysteresis loops varies for each substrate, as do the coercive fields. The coercive fields have been found to be  $\pm 18$  V/ $\mu\text{m}$  for PZT/ITO/glass, +22 and  $-18$  V/ $\mu\text{m}$  for PZT/Ti–Pt/SiO<sub>2</sub>/Si and +35 and  $-20$  V/ $\mu\text{m}$  for PZT/Pt/MgO. The PZT grown on Pt/MgO, Pt–Ti/SiO<sub>2</sub> and ITO/glass shows an offset or asymmetric hysteresis loop, which was confirmed by the differing fields required for poling during domain modification experiments performed on PZT/Pt/MgO.  $\delta_{33}$  values obtained for the PZT thin films investigated range from 50 pm/V for PZT/Pt–Ti/SiO<sub>2</sub>/Si to 40 pm/V for PZT/ITO/glass. © 2002 Elsevier Science Ltd. All rights reserved.

**Keywords:** AFM; Perovskites; Piezoelectric properties; PZT; Sol–gel methods; Substrates; Thin films

## 1. Introduction

Ferroelectric materials such as lead zirconate titanate (PZT  $\text{PbZr}_x\text{Ti}_{1-x}\text{O}_3$ ) have been undergoing increasing study in recent years, as their suitability for use in non-volatile memories and other MEMS applications has been recognised.<sup>1–3</sup> The development of techniques, such as sol-gel, that allow the production of very highly orientated thin film PZT at temperatures compatible with standard Si fabrication techniques has further enhanced this interest.<sup>4,5</sup> For devices to be made successfully the ferroelectric material produced should be high quality with a minimum of rosettes and for many applications highly [111] orientated.

The scale of interest for the grain and domain structures is now sub-micron. Standard analytical techniques do not allow the determination of ferroelectric properties at this scale. The development of atomic force microscopy has allowed the routine evaluation of surface topography of these materials, and in the last few

years a number of additional techniques have been developed. Prime among these for determining the ferroelectric properties of material is piezoelectric atomic force microscopy (P-AFM). P-AFM detects the converse piezoelectric response of the material under investigation and allows the mapping of the ferroelectric domains. The use of an AFM tip as a small and moveable conductive probe has reduced the scale of the study of piezoelectricity to just a few tens of nanometers. Using PFM it is possible to map ferroelectric domains in a film without a top electrode and without altering them.<sup>6–8</sup>

## 2. Experimental

A schematic of the experimental arrangement used to perform PFM is shown in Fig. 1. A sinusoidal signal was passed between the AFM tip and the back electrode of the PZT sample, usually held at ground. The signal used in all cases was 18 kHz and 2 V peak–peak. The resonant frequency chosen was well below the fundamental resonant frequency for the cantilever and 2 V p–p was below the coercive field for the samples under

\* Corresponding author.

E-mail address: [s.c.dunn@cranfield.ac.uk](mailto:s.c.dunn@cranfield.ac.uk) (S. Dunn).

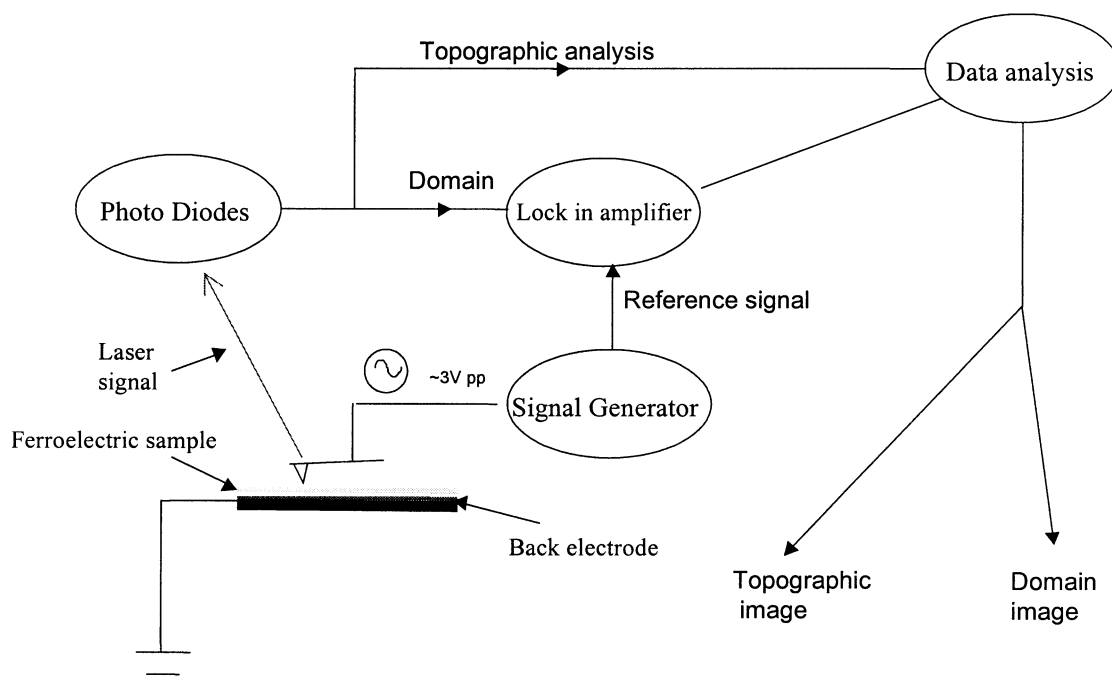


Fig. 1. Schematic of P-AFM experimental arrangement.

evaluation. The converse piezoelectric effect causes a distortion in the shape of the sample due to the external electric field. When completing PFM, a lock-in amplifier is used to filter the distortions due to the converse piezoelectric effect from the bulk topographic signal. In this way it is possible to obtain both topographical and piezoelectric data in one experimental run.

It has also been shown that when a field in excess of the coercive field is applied between the AFM tip and ground the material in that region is poled.<sup>9,10</sup> Using this technique it is possible to manipulate the domain structure in the ferroelectric material. By applying a DC bias in series with the AC signal passed between the tip and ground, it is possible to produce hysteresis loops from localised regions of the material.<sup>11,12</sup> In this paper we use the term  $\delta_{33}$  to describe the response of the ferroelectric film under investigation.

Films were prepared using a sol-gel technique that has been described in earlier work.<sup>4</sup> The films were fired at two temperatures, initially, a pyrolysis temperature of 200 °C for samples fired on Pt back electrodes for 30 s with samples fired on ITO being fired for 2 min at 450 °C. A final phase transformation temperature of 520 °C for samples on Pt with a dwell of 5 min, the ITO samples were fired at 600 °C for 20 min.

A Siemens D5005 system using Bragg-Brentano geometry and  $\text{CuK}\alpha$  radiation was used to perform XRD analysis of the samples.

### 3. Results and discussion

#### 3.1. Topography

Samples of lead PZT(30/70) deposited on Pt/MgO, Pt-Ti/SiO<sub>2</sub> and ITO/glass were examined using tapping mode AFM. Fig. 2 shows the topography for a sample of PZT/Pt/MgO. This sample was very highly [100] orientated, the film consisted of small grains, less than 100 nm in diameter, with a small number of defects. The defects are not clearly seen on the topographic image of the film surface but are readily seen in the piezoresponse P-AFM image. The maximum Z-range for the region investigated was 12 nm, no long range surface features can be seen in the image. Fig. 3 shows the topography obtained for a sample of PZT/Pt-Ti/SiO<sub>2</sub>. The sample was highly [111] orientated and consists of small grains, less than 100 nm in diameter, that appear with-in a larger ordering of the PZT. The maximum Z-range for the sample was 23 nm. The topography of the surface of a PZT/ITO/glass sample, shown in Fig. 4, consists of a small number of large grains that are centred on a single rosette nucleation site. The size of the individual grains varies from between ca. 1 and 2.5  $\mu\text{m}$ , the maximum Z-range for the image is 38 nm. An XRD examination of the PZT on ITO/glass showed that the grains in the PZT layer are randomly orientated.

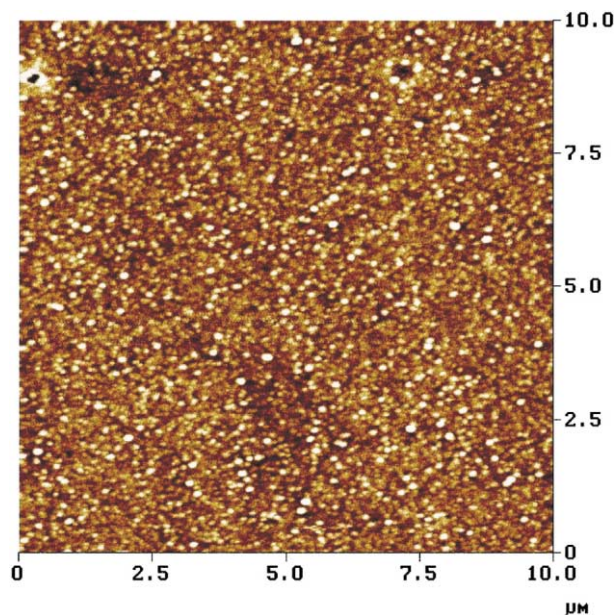


Fig. 2. Tapping mode AFM image for surface of PZT/Pt/MgO.

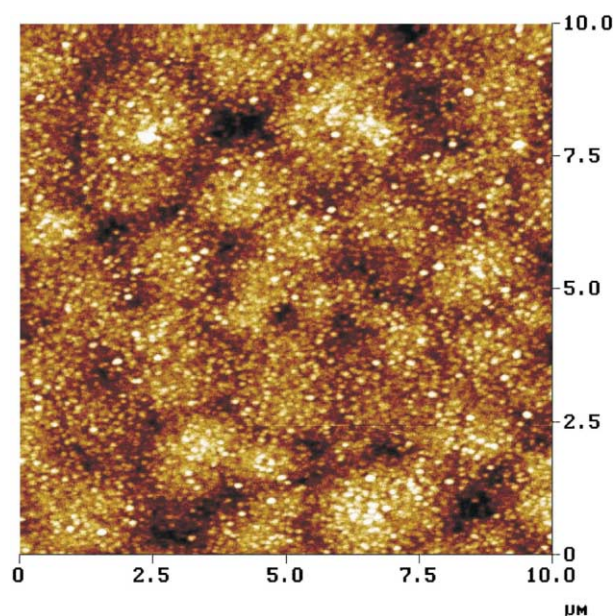


Fig. 3. Tapping mode AFM image for surface of PZT/Pt-Ti/SiO<sub>2</sub>.

The difference in the observed surface microstructure for the PZT samples originates from the nucleation density and subsequent growth of the PZT. The production of a ferroelectric thin film by the metal-organic route consists of a number of steps. In the case of the production of perovskite (piezoelectric) PZT, the sol is first pyrolysed, this forms the non-piezoelectric pyrochlore phase, this is then transformed by high temperature annealing into the piezoelectric perovskite phase. The transformation from pyrochlore to perovskite is dependent on a number of factors and of high significance is the density of suitable sites for the nuclea-

tion of the perovskite phase at the PZT-electrode interface. In the case of a Pt electrode on Ti/SiO<sub>2</sub> the crystallographic lattice mismatch between the PZT and Pt produces a very large number of nucleation sites as does the formation of a transient Pt<sub>3</sub>Pb intermetallic, which significantly reduces the activation energy for phase transformation.<sup>13,14</sup> The orientation of PZT grown depends on the lattice mismatch between the Pt and PZT. In the case of Pt on SiO<sub>2</sub> the PZT grows as a very [111] orientated phase. For Pt/MgO the PZT develops into a very highly orientated [100] structure due to lattice constraints imposed on the Pt by the

MgO. In this case the Pt grows on the surface of the MgO highly orientated in the [100] plane with respect to the surface of the MgO. In both cases this leads to a transformed perovskite phase that consists of a large number of small grains that are highly columnar. The ITO back electrode is nearly completely amorphous with very little crystal structure. Nucleation of the perovskite phase occurs at defect sites and is a function of the drying time and temperature.<sup>15</sup> Subsequent growth of the perovskite phase occurs from the nucleation site and spreads through the pyrochlore phase. The interfaces between two growth regions develop into grain boundaries.

### 3.2. PFM studies

PFM studies were performed on samples of PZT grown on Pt–Ti/SiO<sub>2</sub>, Pt/MgO and ITO/glass. The PFM image obtained for PZT/Pt/MgO is shown in Fig. 5. The image shows that the majority of the grains of PZT are not poled and that the surface has an almost neutral piezoelectric response. The only regions of high response are those around or near the defects in the surface.

The application of an external electric field that is greater than the coercive field of the film will pole the

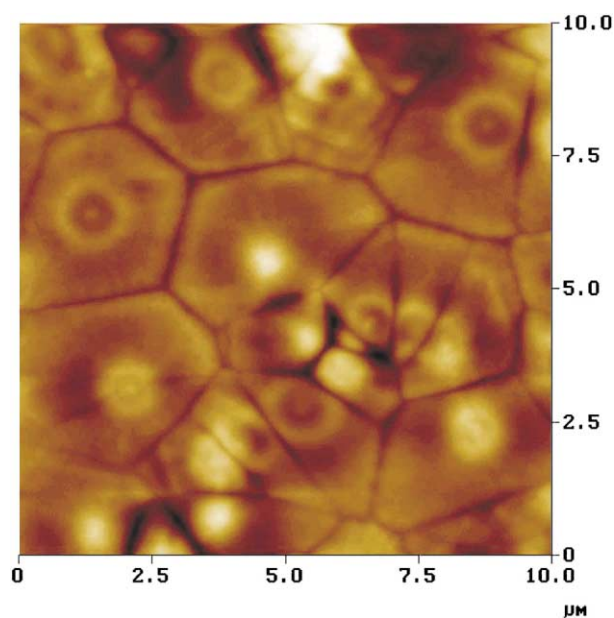


Fig. 4. Tapping mode AFM image for surface of PZT/ITO/glass.

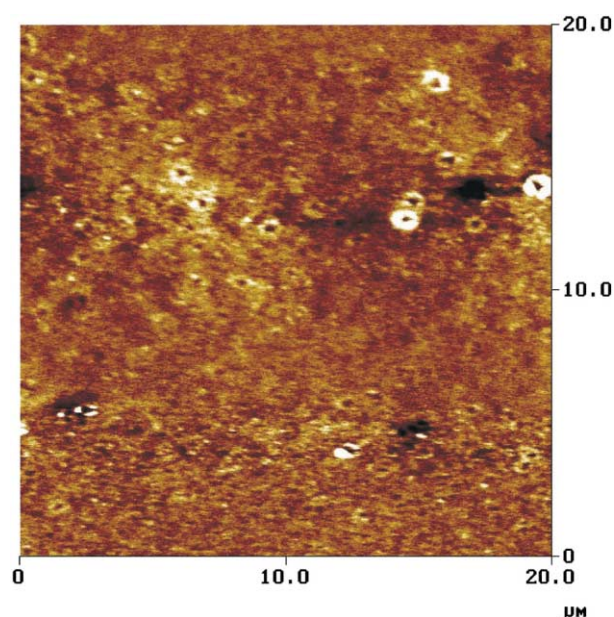


Fig. 5. P-AFM image taken of PZT/Pt/MgO.



sample. Fig. 6 shows the PFM response of the film after a poling experiment. The sample shows excellent poling characteristics, as expected for a highly orientated sample. The larger contrast between the background and black (+ve applied to AFM tip) and white (–ve applied to AFM tip) indicate that the as deposited film forms with an inherent internal electrical bias.

The PFM studies completed for samples of PZT/Pt–Ti/SiO<sub>2</sub> show that the domain structure for the PZT is neutral over the surface of the sample, shown in Fig. 7. Very few regions of defects can be seen and the sample appears to be very homogenous.

By contrast the domain structure for the PZT/ITO/glass structure is very different, as shown in Fig. 8. The structure of the domains within grains and the image as a whole gives a picture that is consistent with the XRD findings of a randomly orientated PZT film. Individual domains can be seen within grains and the grain boundaries are clearly seen. Some grains appear to have a neutral piezoelectric response while others are strongly poled. The application of a field above the coercive field does not result in complete poling. This is a result of the random orientation of the grains which does not allow complete poling, shown in Fig. 9. It is clear that some of

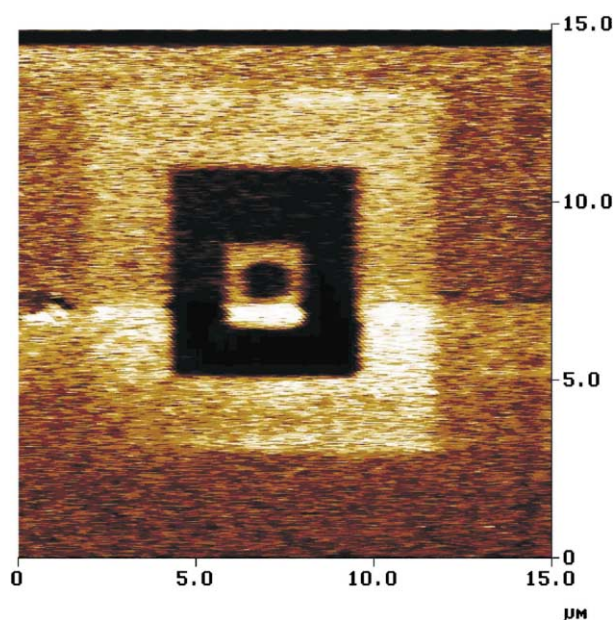


Fig. 6. Post poling image of PZT/Pt/MgO taken with P-AFM.

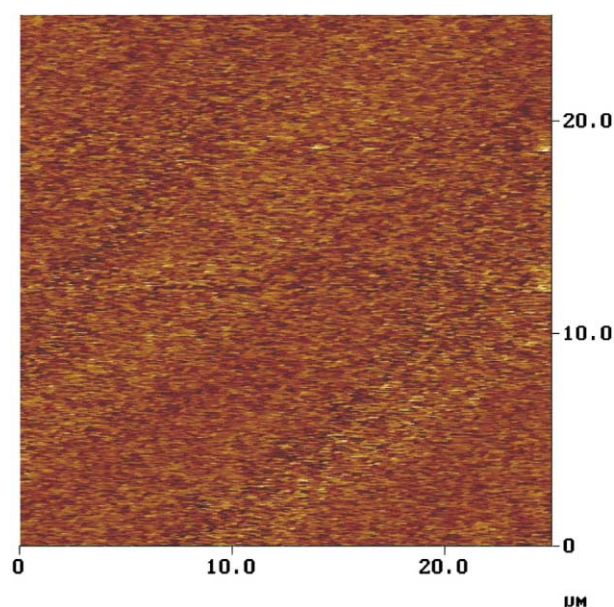


Fig. 7. P-AFM image of PZT/Pt–Ti/SiO<sub>2</sub>.

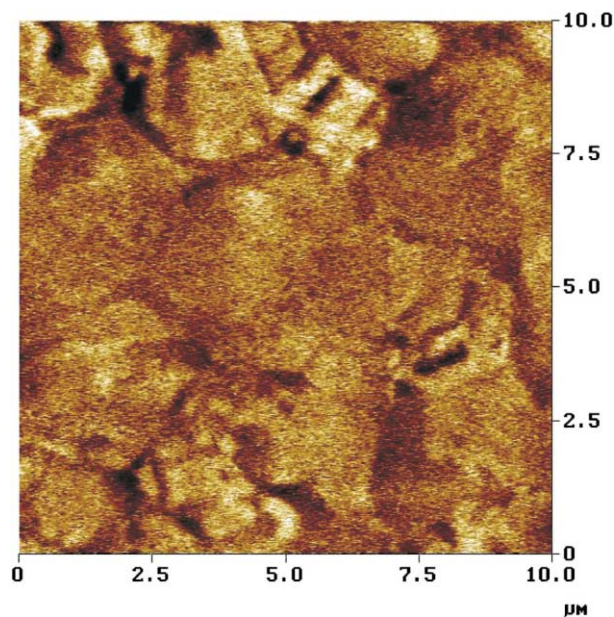


Fig. 8. P-AFM image taken of PZT/ITO/glass.

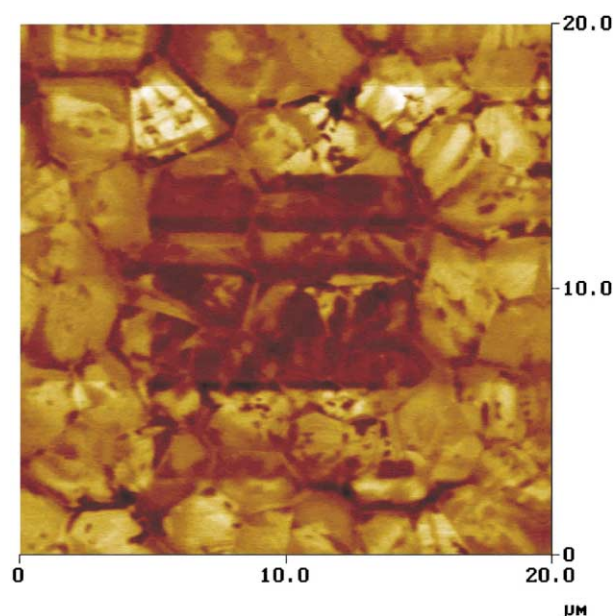


Fig. 9. Post poling image of PZT/ITO/glass taken with P-AFM.

the grains have poled more completely than others and that some regions have not poled at all. This is consistent with a piezoelectric material of random orientation.

### 3.3. Hysteresis loops performed with PFM

Hysteresis loops were performed on the samples using PFM. The hysteresis loops produced for each of the PZT samples tested are shown in Fig. 10. In all cases a typical open hysteresis loop for a piezoelectric material is observed. For the PZT/Pt–Ti/SiO<sub>2</sub> material the  $\delta_{33}$

value obtained using PFM was 62 pm/V. This value is very close to that determined for  $d_{33}$  using a Berlincourt method, of 55 pm/V,<sup>16</sup> and indicates that the  $\delta_{33}$  value returned by the PFM system is close to the  $d_{33,t}$ . The hysteresis loop for PZT/Pt–Ti/SiO<sub>2</sub> has a slight amount of asymmetry with a coercive field of +22 and –18 V/ $\mu$ m. A similar degree of asymmetry has been noticed for samples of PZT/Pt–Ti/SiO<sub>2</sub> when conducting pyroelectric experiments.<sup>17</sup>

The hysteresis loop produced by PZT/Pt/MgO is highly asymmetric on the as grown thin film. The values for the coercive field for the sample are +35 and –20V

$\mu\text{m}$ . The loop produced for PZT/Pt/MgO is not quite as square in shape as the PZT/Pt–Ti/SiO<sub>2</sub> loop. These changes in the shape of the loop are likely to derive from the differences in the crystallographic orientation of the film. Fig. 11, shows the relative orientations of domains in the PZT grown on Pt/MgO and Pt–Ti/SiO<sub>2</sub>. The difference in the orientation of the domain relative to the surface means that in the case of PZT/Pt/MgO the field applied to the surface of the film is all in the correct orientation to re-orientate the domain. In the case of PZT/Pt–Ti/SiO<sub>2</sub> the field applied to the surface does not have the same direct effect on domain re-orientation. The changes in the hysteresis loop shape are exaggerated in the case of PFM due to the very small spatial distribution of field when using the AFM tip as a top electrode.

The hysteresis loop for the PZT/ITO/glass structure is by contrast to PZT grown on Pt symmetrical. The

coercive field for the sample is  $\pm 18 \text{ V}/\mu\text{m}$ . No comment can be made on the shape of the hysteresis loop as this varies depending on where the loop is obtained due the random orientation of the sample. However, in all cases the hysteresis loop obtained for PZT/ITO/glass shows a symmetrical shape.

Asymmetry in the perovskite material has been attributed to the presence of oxygen vacancies pinning domains and a variation in top and bottom electrode. It has also been proposed that oxygen defects at the interface between the ferroelectric material and the electrode causes a built in electrical bias to develop in the film. The variations in hysteresis loop found in the three systems investigated are unlikely to arise from electrode effects as a variation is seen with the same electrode system. Therefore, the changes in hysteresis loop are due to changes in defect density and their location in the film.

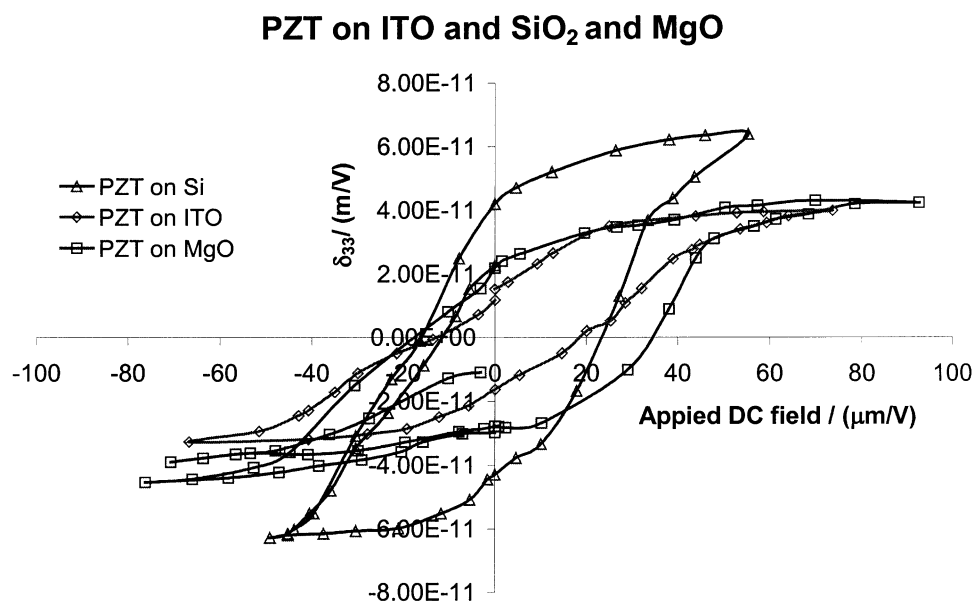


Fig. 10. P-AFM hysteresis loops obtained for PZT on Pt/MgO, Pt–Ti/SiO<sub>2</sub> and ITO/glass.

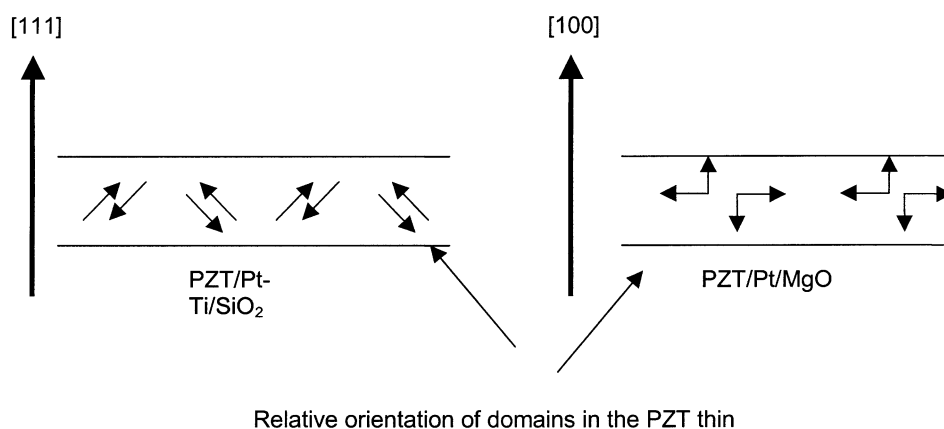


Fig. 11. Orientation of domains relative to surface of sample for PZT grown on Pt/MgO and Pt–Ti/SiO<sub>2</sub>.

### Fatigue of PZT on Pt/MgO and Pt/Ti/SiO<sub>2</sub>/Si

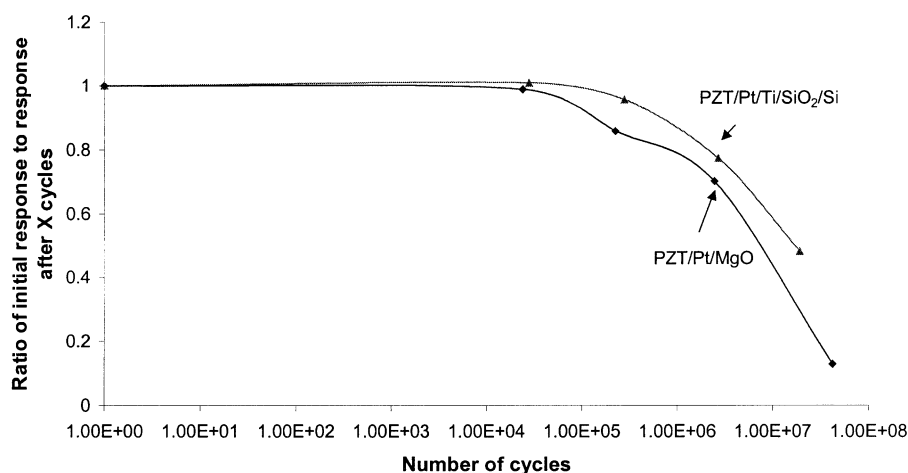


Fig. 12. Fatigue characteristics for PZT/Pt–Ti/SiO<sub>2</sub> and PZT/Pt/MgO.

The amount of oxygen vacancies presents, and hence the inherent electrical bias of the film, is dependent on a number of factors. The other major factor is the interaction of the growing perovskite phase with the electrode system. This interaction occurs at two distinct stages. The first is the interaction of the electrode with the sol as it transforms from pyrochlore into perovskite. The second is whether the film is blocking to oxygen transport or not. It is likely that the different interactions between the sol and the back electrode will affect the defect density at the interface. The presence of Pt allows the formation of Pt<sub>3</sub>Pb, a transient intermetallic phase, which reduces the activation energy for the transformation of the pyrochlore phase to the perovskite phase.<sup>13</sup> The difference in orientation of the Pt electrode system, [111] on SiO<sub>2</sub> and [100] on MgO, may change the activation energy for formation of the perovskite phase. The changes in the crystal structure at the interface may impose additional strain on the PZT grown on [100] Pt over that grown on [111] Pt. It may also alter the amount of oxygen defects formed if the rate of reaction changes, an increase in the number of defects formed would be associated with a slowing of the formation of perovskite PZT. The symmetrical loop for PZT/ITO/glass is due to the availability of oxygen in the ITO. The perovskite PZT is able to scavenge oxygen from the interface between ITO and PZT to produce a film that has no inherent built in charge separation. The trend observed for the symmetry of the hysteresis loops is, with most symmetrical first, PZT/ITO/glass; PZT/Pt–Ti/SiO<sub>2</sub> and then PZT/Pt/MgO.

Fatigue experiments were performed on the samples of PZT/Pt–Ti/SiO<sub>2</sub> and PZT/Pt/MgO. The results are shown in Fig. 12 and show the trend expected for samples with a variation in oxygen defects. The MgO substrate system fatigues more rapidly than the SiO<sub>2</sub>

system, this result supports the view that asymmetry shown in both the PFM surface maps and hysteresis loops is due to oxygen defects and not the difference in top and bottom electrodes.

### 4. Conclusions

PFM, tapping mode AFM and XRD have shown that the substrate used for growth of PZT affects the surface topography and the crystallographic orientation. The orientation of the PZT film is a strong factor on the hysteresis loop produced by the sample and also on the degree of homogeneity found in the poled samples. Samples exhibiting very high crystallographic uniformity show a higher  $\delta_{33}$  than those with a random orientation. The map of piezoelectric response found for highly orientated samples indicates that it is possible to pole the film almost completely. In the randomly orientated sample the piezoelectric map shows that it is not possible to completely pole the sample. The sample is behaving much like a polycrystalline compact. Changes in the symmetry of the hysteresis loop have been found. These changes are due to the availability of oxygen at the electrode PZT interface or the amount of defects formed at the interface. Fatigue experiments have shown that the PZT/Pt/MgO system fatigues more rapidly than the PZT/Pt–Ti/SiO<sub>2</sub> system. This result confirms that the variation in PFM response and hysteresis loop is due to oxygen defects and not the variation in top and bottom electrode.

### Acknowledgements

The authors would like to thank Dr. C. Shaw, Dr. Q. Zhang, Dr. P. Rayner, Mr. A. Stallard, The EPSRC,



TDK Corporation Japan, The Inamori Foundation and the Royal Academy of Engineering.

## References

1. Auciello, O., Scott, J. F. and Ramesh, R., The ability of ferroelectric materials to switch robustly from one polarisation state to another forms the basis of a new thin film technology for storing data. *Physics Today*, 1998, **51**, 22.
2. *Ferroelectric Thin Films VII 29 November–3 December, 1998*. Materials Research Society (MRS), Proceedings published electronically, <http://www.mrs.org/meetings/fall98/program/o.html>.
3. *Ferroelectric Thin Films VIII 28 November–2 December, 1999*. Materials Research Society (MRS), Proceedings published electronically, <http://www.mrs.org/meetings/fall99/progbook/ProgramBookY.html>.
4. Huang, Z., Zhang, Q. and Whatmore, R. W., The role of an inter-metallic phase on the crystallisation of lead zirconate titanate in sol-gel process. *Journal of Materials Science Letters*, 1998, **17**, 1157.
5. Zhang, Q., Huang, Z., Vickers, M. E. and Whatmore, R. W., Effect of the particle size in PZT precursor sols on the orientation of thin films. *Journal of the European Ceramic Society*, 1999, **19**, 1417.
6. Zavala, G., Fendler, J. and Trolier-McKinstry, S., Characterisation of ferroelectric lead zirconate titanate films of scanning force microscopy. *Journal of Applied Physics*, 1997, **81**, 7480.
7. Eng, L. M., Abplanalp, M., Gunter, P. and Guntherodt, H. K., Ferroelectric domains studied by Piezoresponse AFM. *Journal of Physics IV France*, 1998, **8**, Pr9–201.
8. Franke, K., Besold, J., Haessler, W. and Seegebarth, C., Ferroelectric domain structures studied by piezoresponse scanning force microscopy. *Surface Science Letters*, 1994, **302**, L283.
9. Guthner, P. and Dransfield, K., Local poling of ferroelectric polymers by scanning force microscopy. *Applied Physics Letters*, 1992, **61**(9), 1137.
10. Hidaka, T., Maruyama, T., Sakai, I., Saitoh, M., Wills, L. A., Hiskes, R., Dicarolis, S. A., Amana, J. and Foster, C. M., *Integrated Ferroelectrics*, 1997, **17**, 319.
11. Dunn, S. and Whatmore, R. W., An examination of thin film lead scandium tantalum oxide (PST) using piezoAFM. *Journal of Material Science Letters*, 2001, **20**, 179.
12. Takada, K., Strain imaging of a Pb(Zr,Ti)O<sub>3</sub> thin film. *Journal of Applied Physics*, 1996, **79**(1), 134.
13. Wilson, R., Huang, Z., Zhang, Q., Whatmore, R. W. and Wang, P., Effects of alloying platinum bottom electrode with silver: in relation to CFD processing of PZT thin films. *Integrated Ferroelectrics*, 2000, **29**, 251.
14. Huang, Z., Zhang, Q. and Whatmore, R. W., Structural development in the early stages of annealing of sol-gel prepared lead zirconate titanate thin films. *Journal of Applied Physics*, 1999, **86**(3), 1662.
15. Roy, S. S., Gleeson, H., Shaw, C. P., Whatmore, R. W., Huang, Z., Zhang, Q. and Dunn, S., Growth and characterisation of lead zirconate titanate (30/70) on indium tin oxide coated glass for oxide ferroelectric-liquid crystal display application. *Integrated Ferroelectrics*, 2000, **29**, 189.
16. Southin, J., Wilson, S. and Whatmore, R.W.,  $E_{31,f}$  Determination of PZT films using a conventional ' $d_{33}$ ' meter. *Journal of Physics D, Applied Physics*, in press.
17. Zhang, Q. and Whatmore, R. W., Pyroelectric properties of sol-gel PZT and Mn doped PZT thin films. Results presented at ISIF 2001, Colorado Springs, Colorado, 10–14 March 2001.